JOURNAL OF MATERIALS SCIENCE **37** (2002) 3397–3403

Synthesis and processing of nanostructured WC-Co materials

Z.-G. BAN, L. L. SHAW
Department of Metallurgy and Materials Engineering, Institute of Materials Science, University of Connecticut, Storrs, CT 06269, USA
E-mail: lshaw@mail.ims.uconn.edu

In this study a novel approach, termed the integrated mechanical and thermal activation (IMTA) process, was used to synthesize nanostructured WC-Co powder. As a result of the integration of mechanical and thermal activation, nanostructured WC-Co powder was synthesized below 1000°C, starting from WO_3, CoO and graphite powder mixtures. Furthermore, consolidation of the nanostructured WC-Co powder via high velocity oxy-fuel (HVOF) thermal spraying and solid state sintering was investigated. The results demonstrated the feasibility of converting the nanostructured WC-Co powder to coatings and bulk components, the properties of which are either comparable to or better than that of the conventional coarse-grained counterparts.

1. Introduction

As a result of extremely fine microstructure, nanostructured materials have long been recognized to have remarkable and technologically attractive properties [1]. On one hand, ultrafine grains can endow the material with improved hardness and strength, as anticipated from the well-known empirical Hall-Petch relationship; on the other hand, the increased volume fraction of grain boundaries may enhance the toughness and ductility of the material. For this reason, higher hardness has been achieved in nanostructured materials, such as WC-Co cermets, without degradation of the toughness [2]. WC-Co is a technologically important composite material and has been widely used as cutting tools, rock drills, punches and wear-resistant coatings [3]. Thus, realization of the potential of nanostructured WC-Co materials will have technological and economical impacts on industry. This turns out to be one of the driving forces for the fast growing technologies for synthesizing nano-phase WC/Co powder, such as mechanical alloying [4, 5] and chemical processing [6, 7].

The integrated mechanical and thermal activation (IMTA) process has been developed as a viable technique for producing large quantities of nanostructured carbides (e.g. SiC and TiC) [8–11] and nitrides (e.g. Si_3N_4, CrN and TiN) [12–14]. This new process combines mechanical and thermal activation to enhance the formation of carbides and nitrides. The basic form of the IMTA process is to mechanically activate reactants (usually a mixture of oxide and graphite powder) at room temperature through high energy milling (the mechanical activation step), followed by completing the synthesis reaction at high temperatures (the thermal activation step). Because of the mechanical activation at ambient temperature, the synthesis reaction of the IMTA process can be carried out at much lower temperatures and/or shorter time than those used in the conventional method for making coarse-grained carbides and nitrides. This in turn leads to the formation of nanostructured nitrides and carbides.

In this article, we describe highlights of synthesizing nanostructured WC-Co powder using the IMTA process. The method for obtaining nano-phase WC-Co powder with no free carbon or a controlled amount of free carbon has been studied. The feasibility of consolidating the nano-phase WC-Co powder using thermal spraying and solid state sintering has also been investigated.

2. Experimental procedures

The starting materials for preparing the powder mixture were tungsten trioxide (WO_3) powder (99.8%, 10–20 micrometers), graphite powder (99.9%, −100 mesh) and cobalt oxide (CoO) powder (99%, −325 mesh). The powder mixture prepared contained WO_3, C and CoO with a molar ratio of 1:2.4:0.7 in order to form a final product of WC + 18wt%Co + 5.3wt%C. This powder mixture was high energy milled for different times using a modified Szegvari attritor [15] in argon. The canister of the attritor was made of a stainless steel and the charge, consisting of WC balls with a diameter of 4.76 mm and the powder mixture, was agitated by WC arms radiating from a central rotating WC-coated stainless steel shaft. The ball-to-powder weight ratio was 60:1 and a milling speed of 600 RPM was employed.

The mechanically activated (high energy ball milled) powder was subsequently subjected to thermal activation. Thermal activation was carried out by heating the milled powder at 650°C for 2 h in a gas mixture of H_2 ($P_{H_2} = 0.5$ atm) and Ar ($P_{Ar} = 0.5$ atm), followed by ramping to 1000°C and holding at this temperature for

2 h in pure argon ($P_{Ar} = 1.0$ atm). As will be shown later, free carbon is often present in the nanostructured WC-Co powder obtained from the IMTA process because of the extra carbon added at the beginning of the process. Furthermore, free carbon may be needed for thermal spraying of WC-Co coatings (to be discussed more in Section 3.2). Thus, to control the free carbon concentration in the as-synthesized WC-Co powder, a gas mixture of CO/CO_2 was used to purify the powder at a chosen temperature after the thermal activation.

To investigate the feasibility of consolidating the resulting nano-phase WC-Co powder, high velocity oxy-fuel (HVOF) thermal spraying and free sintering were used to prepare coatings and bulk samples respectively. Before thermal spraying the nano-phase powder was agglomerated using methyl cellulose in order to satisfy the particle size requirement in thermal spraying. WC-Co coatings were sprayed on a blasted mild steel surface with a Jet-Kote spraying gun. Hydrogen was used as the fuel gas with argon as the powder carrier gas. Other spraying parameters can be found in Table I. The bulk WC-Co samples were obtained by uniaxial cold pressing of the nano-phase powder, followed by free sintering at 1280°C for 2 hours in an argon atmosphere.

Phase identification in the as-synthesized powder and the consolidated samples was carried out employing X-ray diffraction (XRD) with Cu K_α radiation (Bruker Axs D5005D X-ray Diffractometer). The average grain sizes of the powder and the consolidated samples were estimated based on XRD peak broadening using the Scherrer formula with consideration of internal strain [16]. The grain size of the nano-powder was also examined using an analytical transmission electron microscope (TEM, Philips EM420). The carbon content in the WC-Co powder was determined using the carbon determinator (mode WR-12 LECO Corp.). Morphology of the powder was examined utilizing SEM (Philips, ESEM 2020). The densities of the sintered samples were measured on the basis of Archimedes's principle [17]. Vickers microhardness tests were performed on both sintered samples and coatings using a LECO DM-400FT hardness tester with a 300-g load and a dwell time of 20 seconds. The microhardness value reported is the average of 5 indentations.

TABLE I Parameters employed during HVOF spraying

Spray parameter	Value
Powder feed rate	20 g/min
Spraying distance	20.3 cm
Oxygen pressure	0.689 MPa
Hydrogen pressure	0.689 MPa
Ratio of O_2 to H_2 flow rate	0.5

3. Results and discussion

3.1. Powder synthesis

Fig. 1 shows XRD patterns of the powder mixture before milling and milled for different times at ambient temperature. It can be seen that the starting materials of WO_3, CoO and graphite are crystalline. With the increase of milling time, some distinct features can be identified. First, the intensity of graphite peaks was substantially reduced in 6-hours of milling, which is believed to be caused by the amorphization of graphite [15]. Second, the intensity of WO_3 peaks decreases with increasing of milling time and the remaining reflections of WO_3 exhibit broadening, suggesting the reduced crystallite size and/or the introduction of the internal strain due to ball milling. Third, the peak broadening and intensity decrease also occur for CoO, again suggesting the reduced crystallite size and/or the introduction of internal strains.

SEM images of the starting and milled powder mixtures are shown in Fig. 2. It can be seen that the sizes of WO_3, CoO and C powders are all reduced to the submicrometer range in just 3 hours of milling, that is, a reduction of particle size from about 40 μm to

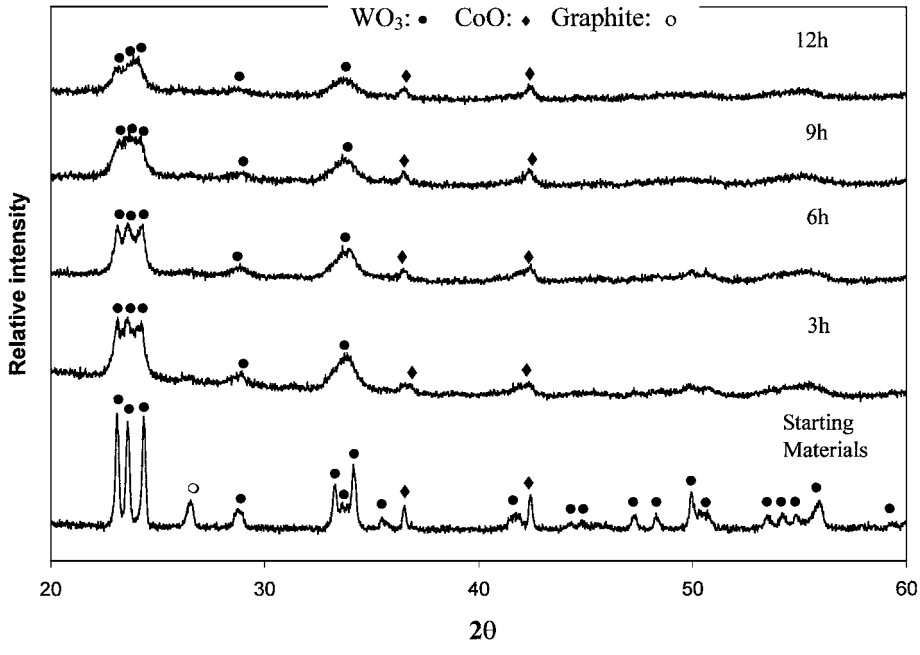

Figure 1 XRD patterns of powder mixture milled for various times in argon.

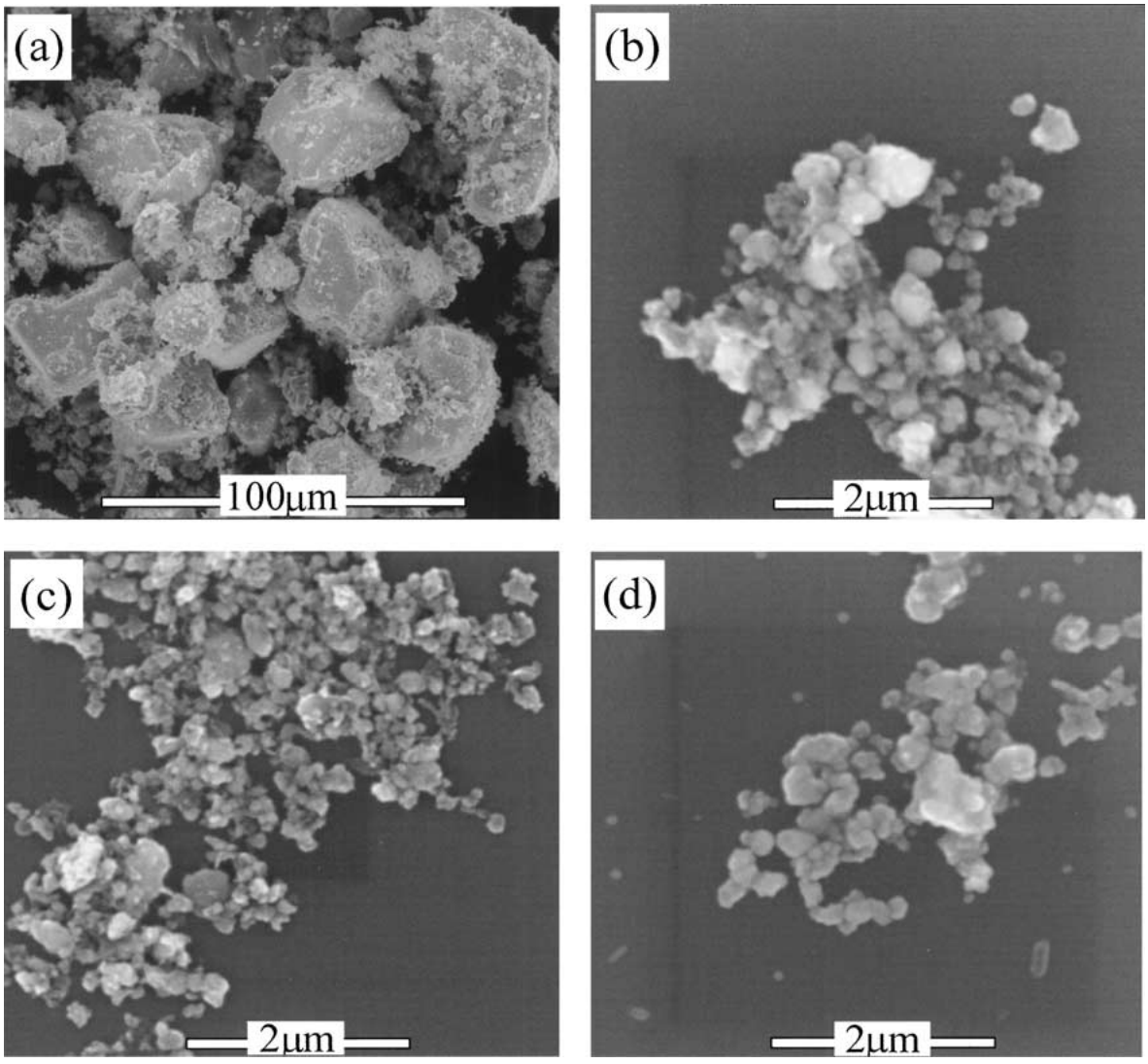

Figure 2 SEM images of WO_3-CoO-graphite powder mixtures with (a) no milling, (b) milling for 3 hours, (c) 6 hours, and (d) 12 hours.

0.3μm. However, beyond the 3 hours of milling little change in the particle size occurs as shown in Fig. 2. The crystallite size of WO_3 in the powder mixture as a function of milling time was estimated according to peak broadening of the XRD pattern and is presented in Fig. 3. It can be seen that the crystallite size of WO_3 has reached nanometer scales with only 3 hours of milling and changed little beyond 9 hours of milling.

From the XRD and SEM examination we can, therefore, conclude that the powder mixture with high energy milling has fine particle sizes, large specific surface areas, amorphous carbon and a higher free energy due to the smaller crystallite sizes and internal strain than the powder mixture prior to milling. These features can significantly enhance the reaction kinetics via increased diffusivities and reaction areas. Furthermore, these features may also increase the reactivity of the reactants by increasing their free energies, as we recently found in synthesizing nanostructured SiC powder using the IMTA process [18]. Thus, this mechanically activated powder mixture is very suitable for the subsequent low temperature thermal activation that will generate nanostructured WC-Co.

The thermal activation consists of two sequential reaction stages; one being the reduction of WO_3 to W and the other the carburization of the reduced powder.

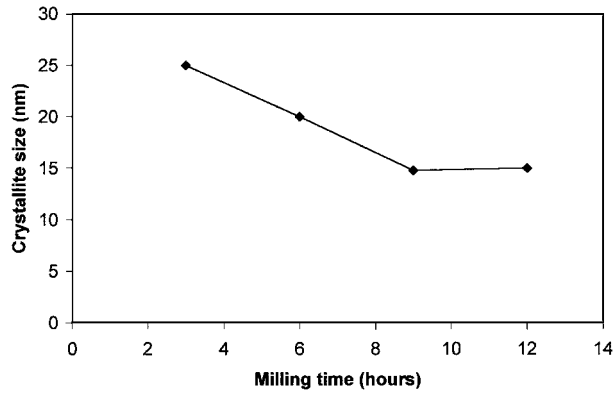

Figure 3 The crystallite size of WO_3 in the powder mixture as a function of milling time.

Fig. 4 is XRD patterns of the powder mixture milled for 6 h, followed by annealing at 650°C for 2 h in a gas mixture of H_2 and Ar ($P_{H_2} = P_{Ar} = 0.5$ atm), then holding at 1000°C for 2 h in pure Ar ($P_{Ar} = 1.0$ atm). It can be seen from Fig. 4a that WO_3 has been completely reduced to W at 650°C, which is lower than the temperature used in the reduction stage of the conventional process for making coarse-grained WC [19]. Based on the peak broadening, the average crystallite size of W is estimated to be about 18 nm, suggesting that the

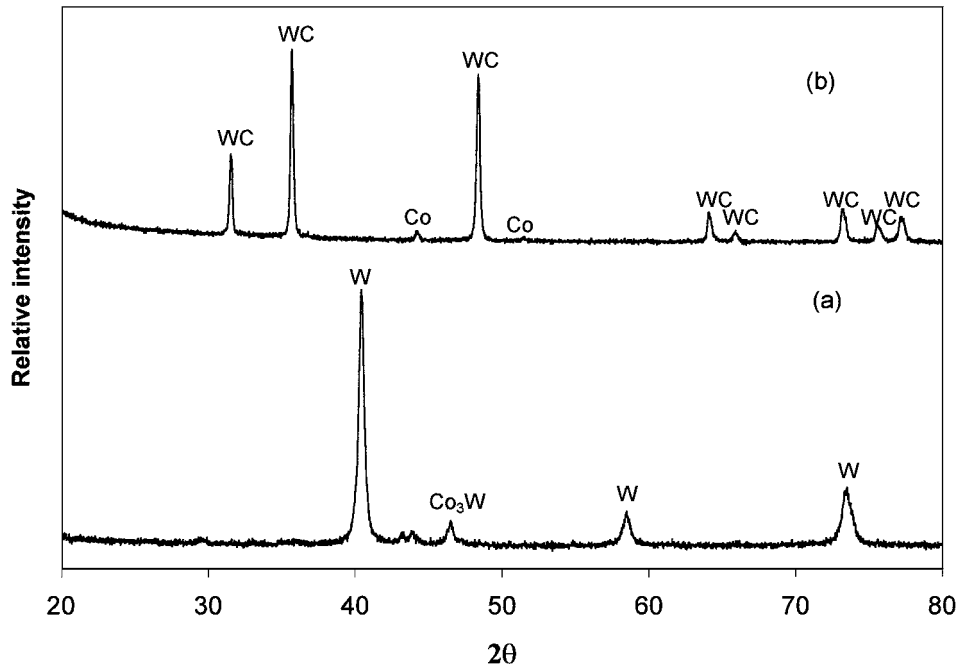

Figure 4 XRD patterns of the powder mixture milled for 6 h, followed by (a) annealing at 650°C for 2 h in the gas mixture of H_2 and Ar ($P_{H_2} = P_{Ar} = 0.5$ atm), and (b) subsequently holding at 1000°C for 2 h in pure Ar ($P_{Ar} = 1.0$ atm).

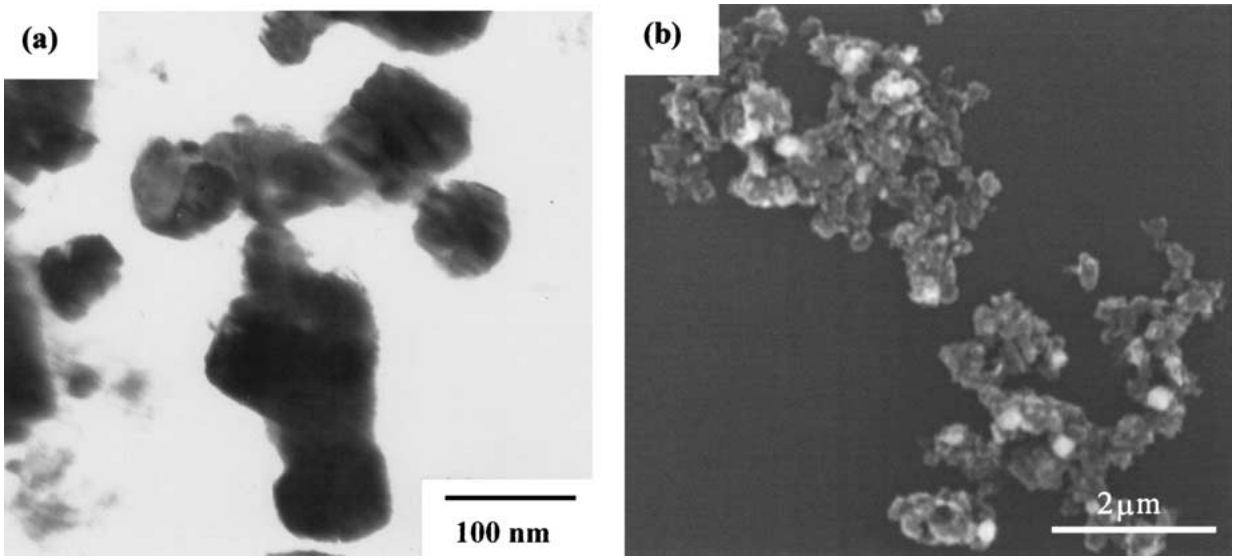

Figure 5 (a) TEM and (b) SEM image of the as-synthesized WC-Co powder, showing nanometer-sized grains within submicrometer-sized particles.

fine-scale microstructure in the as-milled powder is retained in the reduced powder. Interestingly, an intermediate compound Co_3W is formed in the reduction stage, which is not reported in any other synthesis routes. The reduced powder can be fully converted to WC-Co at 1000°C in a pure argon atmosphere, as indicated in Fig. 4b. All the peaks can be attributed to WC and Co, and there are no complex carbide phases detectable in the XRD pattern. Again, based on the peak broadening the crystallite size of the WC formed is estimated to be around 30 nm, which is confirmed by the TEM examination as shown in Fig. 5a. The general morphology of the WC-Co powder obtained is shown in Fig. 5b which reveals that the particle size of the WC-Co powder is in the range of 0.3 to 0.5 micrometers. Thus, the WC-Co powder prepared from the IMTA process has submicrometer-sized particles with nanoscale grains.

The typical carburization temperature in the conventional process for making coarse-grained WC-Co powder is in the range of 1400–1600°C [20]. Our results clearly show that the carburization temperature required to fully convert the reduced powder to WC-Co is much lower than that in the conventional process. Accordingly, it is reasonable to suggest that the key factor enabling the formation of the nanostructure is the low WC formation temperature at which the grain growth can be inhibited significantly. The low formation temperature is made possible through the mechanical activation prior to the thermal activation. The latter is also necessary because WC and Co cannot be formed by prolonged milling of WO_3, CoO and C mixtures at ambient temperature. Thus, because of the integration of the mechanical and thermal activation nanostructured WC-Co can be prepared from low

cost materials at low temperatures with short processing times. The IMTA process, therefore, offers a promising cost-effective approach for large-scale fabrication of nanostructured WC-Co powder.

3.2. Control of free carbon concentration in nano-phase WC-Co powder

Free carbon is always a concern in making bulk cemented carbides and thermally sprayed coatings. Free carbon is generally considered detrimental to the mechanical properties of sintered WC-Co since the presence of free carbon reduces the hardness and wear resistance. However, it is found that in thermal spraying an addition of small amounts of graphite to the starting WC-Co powder may suppress the WC decomposition to a certain extent [21, 22]. Thus, it is necessary to adjust the free carbon concentration in nano-phase WC-Co powder, depending on the application desired. Free carbon is often present in the nanostructured WC-Co powder obtained using the IMTA process because of the extra carbon added at the beginning of this process. In order to fully realize the potential of the IMTA process for making sinterable and sprayable nanostructured WC-Co powder, we have utilized a gas mixture of CO and CO_2 to control the amount of free carbon. As will be shown below, the free carbon concentration in the nanostructured WC-Co powder can be controlled by subjecting the as-synthesized nano-powder to a CO/CO_2 treatment.

Fig. 6 shows the domain of existence for pure W_2C, pure WC and WC with free carbon that were calculated assuming the following reactions:

$$C + CO_2 = 2CO \quad (1)$$

$$2WC + CO_2 = W_2C + 2CO \quad (2)$$

The thermodynamic data were obtained from Ref. [23]. The shaded region in Fig. 6 gives the suitable combination of the partial pressure of CO ($P_{CO} + P_{CO_2} = 1.0$ atm) and temperature for eliminating the free carbon without decarburization of WC to W_2C. This theoretical prediction was confirmed by experiment. Fig. 7 shows weight percentage of free carbon as a function of annealing time at 740°C in a gas mixture of CO and CO_2 with $P_{CO} = P_{CO_2} = 0.5$ atm. This condition is located in the middle of the shaded area, as

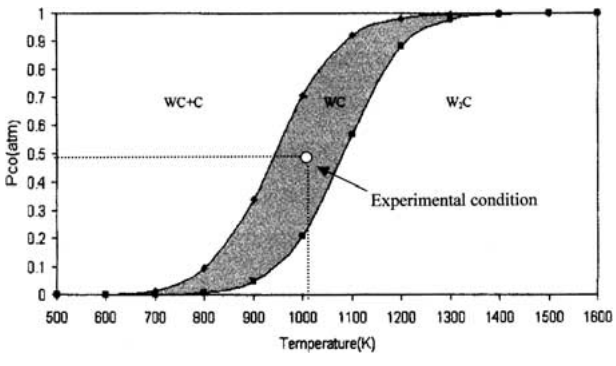

Figure 6 Domains of existence for pure WC, W_2C and WC with free carbon. The open dot marked in the map is the experimental condition used to reduce the free carbon concentration in the powder mixture.

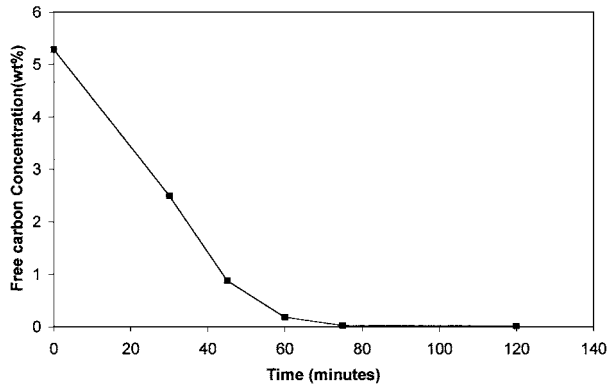

Figure 7 Weight percentage of free carbon in the WC-Co powder as a function of annealing time at 740°C in a gas mixture of CO and CO_2 ($P_{CO} = P_{CO2} = 0.5$ atm).

marked in Fig. 6. The initial free carbon concentration in the as-synthesized WC-Co powder is 5.4 wt%, and nearly all the free carbon is gasified within 75 minutes. This result suggests that nano-phase WC-Co powder with various levels of free carbon can be obtained by adjusting the duration of the CO/CO_2 treatment.

3.3. Thermal spraying of nano-phase WC-Co

High velocity oxy-fuel (HVOF) thermal spraying is the most common spraying technique used for preparing WC-Co coatings because HVOF spraying has been proved to be a better method than air plasma spraying (APS) for retaining a larger fraction of WC and reducing porosity in WC-Co coatings. This is widely attributed to lower temperatures and higher kinetic energy experienced by the powder particles in HVOF compared with APS [24, 25]. In this study the powder feedstock containing 5 wt% free carbon is chosen for the HVOF thermal spray evaluation. Fig. 8 shows the XRD pattern of the powder before thermal spraying and the as-sprayed coating. It is clear that before thermal spraying, only WC and Co peaks are detectable in the powder. However, additional crystalline reflections, corresponding to W_2C and W phases, are present in the coating, suggesting the occurrence of decarburization during thermal spraying. Another distinct feature of the XRD pattern for the coatings is the absence of the Co phase. Moreover, the XRD pattern of the coating exhibits a broad diffraction halo between 2θ values of approximately 37° and 47°. It has been reported that this broad, shallow peak is associated with the formation of amorphous and/or nanocrystalline phases containing tungsten, cobalt and carbon [26–29]. The fact that the cobalt peaks are detected in the powder particles and not in the coating suggests that most of the cobalt in the coating is retained in the amorphous and/or nanocrystalline phases.

Calculation of the coating grain size on the basis of the peak broadening of the XRD pattern suggests that the WC grain size increases slightly during thermal spraying, that is, an increase from 30 nm in the powder to 45 nm in the coating. This is consistent with the fact that the powder particles experience low temperatures and a short dwell time during HVOF thermal spraying. Both low temperatures and short dwell times help

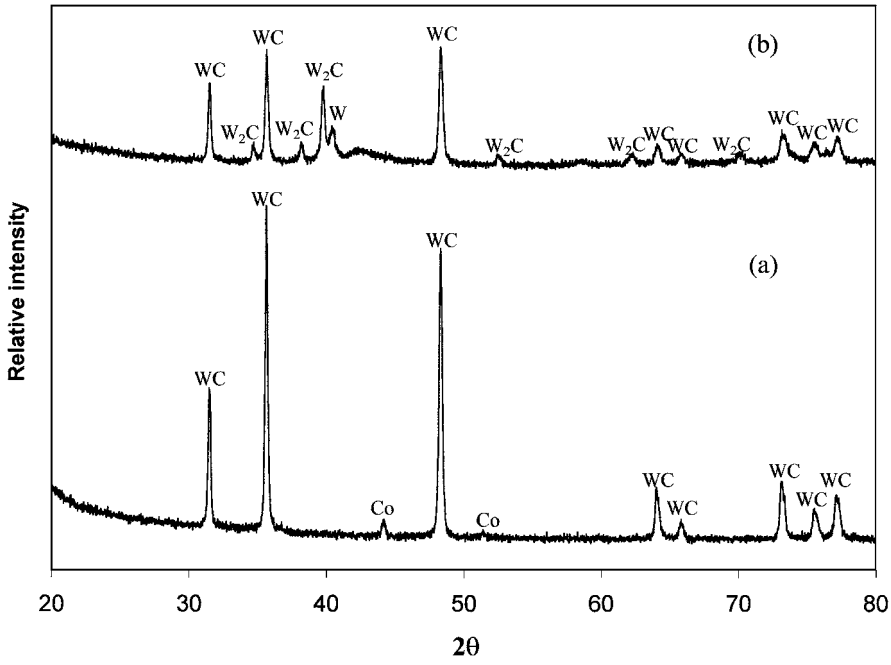

Figure 8 XRD patterns of (a) the powder and (b) the as-sprayed coating.

to preserve the nanocrystalline structure in the final coating [29].

The Vickers microhardness of the as-sprayed coating exhibits an average value of 10.56 GPa (HV_{300g}). This result is comparable to that of the conventional or nanostructured WC-Co coatings reported from the literature [30, 31]. The factors that determine coating hardness are complex and the volume fraction of the retained WC is generally considered to be one of the most important factors [29]. During thermal spraying, WC particles could undergo decarburization, resulting in the reduction of the volume fraction of the WC phase. The nanocomposite powder is expected to suffer greater levels of decarburization than the conventional coarse-grained powder because of the higher surface area per unit volume of particles. Accordingly, less WC is expected to retained in the nanostructured coating unless different thermal spraying conditions are used. The fact that the Vickers hardness of the nanostructured coatings obtained in this study is comparable to that of the conventional coarse-grained coatings may result from a combination of fine grain sizes (∼45 nm) and the low volume fraction of the retained WC phase in the nanostructured coatings. The low volume fraction of the retained WC phase could cancel the benefit of the small grain size. For this reason, optimization of the thermal spraying process is required if the potential of the nanostructured WC-Co coatings is to be realized. Nevertheless, the current results indicate that the nano-phase WC-Co powder synthesized by the IMTA process can be used as powder feedstock for generating nanostructured coatings.

3.4. Powder consolidation via sintering

To further extend the application of the nano-phase WC-Co powder, the sinterability of this powder has been investigated. The sinterability of WC-Co can be influenced by many factors among which the carbon content is often emphasized. On one hand, low carbon content would result in the difficulty of maintaining stoichiometric WC, thereby leading to the formation of the η phase (e.g. Co_3W_3C and Co_6W_6C). On the other hand, an excess of carbon results in the presence of free carbon which would affect the sintering process. Furthermore, the presence of η phase and free carbon is detrimental to mechanical properties of sintered WC-Co [20]. Thus, the nano-phase WC-Co powder for sintering application should be stoichiometric. By using the CO/CO_2 treatment, the concentration of free carbon in the nano-powder has been kept below 0.05 wt% for the sintering application. The preliminary study on sinterability has focused on free sintering of the nano-phase powder without addition of grain growth inhibitors. The relative densities of green bodies and sintered samples (A and B) are given in Fig. 9. It shows that rapid densification of the nano-phase WC-Co powder can occur at 1280°C, which is 40°C below the eutectic temperature of the corresponding W-Co-C system. This is consistent with the concept that nanomaterials can be sintered at lower temperatures than that used for coarse-grained powders [32]. It is also noted that the final density exhibits strong dependence on the green body density. Fully dense WC-Co sample is achieved from a green body which has a high relative density (∼65% of the theoretical density), while the green body with 38% of the theoretical only leads to a sintered body with a 95% of the theoretical density.

The average Vickers microhardness of Sample B (WC-18wt%Co) is 14.71 GPa (HV_{300g}). This value is substantially higher than that of the conventional coarse-grained bulk WC-20wt%Co (10.3 GPa) reported by Jack [3] and WC-15wt%Co (10.5 GPa) prepared from mechanical alloyed WC-Co powder by Mi and Courtney [4]. In fact, the hardness of Sample B is comparable to that of WC cermets that contain less Co such as WC-10wt% Co reported by Jack (15.94 GPa) [3] and Jia *et al.* (12.55 GPa) [2]. SEM examination of

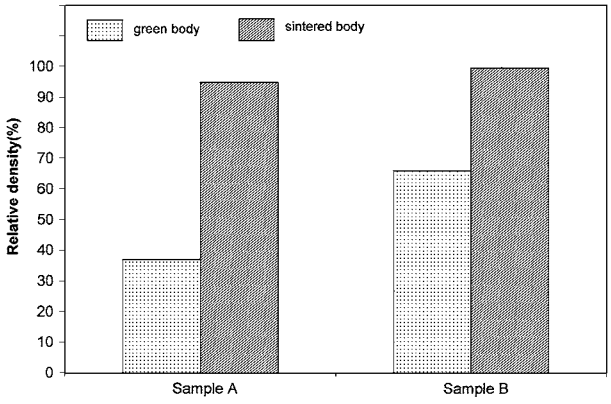

Figure 9 Relative densities of WC-Co green bodies and bulk samples sintered at 1280°C for 2 hours.

the microstructure has revealed that the WC grain size has increased to 0.9 μm during the sintering. The rapid grain growth may be controlled by addition of grain growth inhibitors, such as VC, Cr_3C_2, TaC or their combinations [33], or by conducting the sintering at lower temperatures with the aid of hot isostactic pressing [34]. With the control of grain growth, it is reasonable to expect that further improvements in microhardness can be achieved for the nanostructured WC-Co bulk parts. Hence, the current results clearly demonstrate the potential of converting the nano-phase WC-Co powder synthesized via the IMTA process to hard metals with improved properties.

4. Concluding remarks

Nanostructured WC-Co powder has been successfully synthesized using an integrated mechanical and thermal activation process. The resulting powder has a narrow particle size distribution (0.3–0.5 μm) and the crystallite size of the WC phase is about 30 nm. The feasibility of consolidating the nano-phase powder using high velocity oxy-fuel (HVOF) and solid state sintering has been demonstrated. The average Vickers microhardness of the thermally sprayed coatings is 10.56 GPa (HV_{300g}), which is comparable to that of the conventional coarse-grained WC-Co coatings. Fully dense WC-18wt%Co bulk samples with an average Vickers microhardness of 14.71 GPa (HV_{300g}) has been obtained via solid state sintering of the nano-phase powder. This hardness value is substantially higher than that of conventional WC-20wt%Co materials and comparable to the hardness of conventional WC-10wt%Co materials. These results demonstrate the feasibility of converting the nano-phase WC-Co powder synthesized via the IMTA process to coatings and bulk components, the properties of which are either comparable to or better than that of the conventional coarse-grained counterparts. Since optimization of the consolidation condition has not been carried out yet, it is expected that further improvements in mechanical properties are possible with optimization of processing conditions.

Acknowledgments

This work was supported by the National Science Foundation under grant No: DMR-9710265.

References

1. H. GLEITER, *Nanostruct. Mater.* **1** (1992) 1.
2. K. JIA and T. E. FISCHER, *Wear* **200** (1996) 206.
3. D. H. JACK, in "Engineering Application of Ceramic Materials" (ASM International, Materials Park, OH, 1985) p. 147.
4. S. MI and T. H. COURTNEY, *Scripta Mater.* **38**(1) (1998) 171.
5. M. SHERIF EI-ESKANDARANY, M. OMORI, M. ISHIKURO, T. J. KONNO, K. TAKADA, K. SUMIYAMA, T. HIRAI and K. SUZUKI, *Metall. Mater. Tans.* **27A**(12) (1996) 4210.
6. Y. T. ZHU and A. MANTHIRAM, *J. Amer. Ceram. Soc.* **77**(10) (1994) 2777.
7. B. H. KEAR and L. E. McCANDISH, *Nanostruct. Mater.* **3** (1993) 19.
8. L. L. SHAW, R.-M. REN and Z.-G. YANG, US Patent no. 6,214,309.
9. R.-M. REN, Z.-G. YANG and L. L. SHAW, *Ceram. Eng. Sci. Proc.* **19**(4) (1998) 461.
10. *Idem.*, *Scripta Mater.* **38**(5) (1998) 735.
11. L. L. SHAW, *Adv. Eng. Mater.* **2**(11) (2000) 721.
12. L. L. SHAW, Z.-G. YANG and R.-M. REN, *J. Amer. Ceram. Soc.* **81**(3) (1998) 760.
13. R.-M. REN, Z.-G. YANG and L. L. SHAW, *Nanostruct. Mater.* **11**(1) (1999) 25.
14. *Idem.*, *Mater. Sci. Eng.* A **286** (2000) 65.
15. Z.-G. YANG and L. L. SHAW, *Nanostruct. Mater.* **7**(8) (1996) 873.
16. L. L. SHAW, Z.-G. YANG and R.-M. REN, *Mater. Sci. Eng.* A **244** (1998) 113.
17. S. K. BHAUMIK, G. S. UPADHYAYA and M. L. VAIDYA, *J. Mater. Sci.* **27** (1992) 1947.
18. R.-M. REN, Z.-G. YANG and L. L. SHAW, *J. Amer. Ceram. Soc.* **85** (2002) 819.
19. B. ARONSSON and H. PASTOR, in "Powder Metallurgy: An Overview" (The Institute of Metals, London, 1991) p. 312.
20. S. YIH and C. WANG, in "Tungsten: Source, Metallurgy, Properties and Applications" (Plenum Press, New York, 1979) p. 385.
21. H. L. DE VILLIERS LOVELOCK, *J. Therm. Spray Technol.* **7**(3) (1998) 357.
22. Y. ARATA, A. OHMORI and E. GOFUKU, *Transactions of JWRI* **14**(2) (1985) 67.
23. O. KNACKE, O. KUBASCHEWSKI and K. HESSELMANN (eds.), in "Thermochemical Properties of Inorganic Substances" (Springer-Verlag, Berlin, Germany, 1991).
24. J. NERZ, B. KNSHNER and A. ROTOLICO, in "Protective Coatings: Processing and Characterization," edited by R. M. Yaxici (TMS, Warrendale, PA, 1990) p. 135.
25. J. R. FINCKE, W. D. SWANK and D. C. HAGGARD, in "Proceedings of the 7th national Thermal Spray Conference," edited by C. C. Berndt and S. Sampath (ASM International, Materials Park, OH, 1994) p. 325.
26. C.-J. LIU, A. OHMORI and Y. HARADA, *J. Mater. Sci.* **31** (1996) 785.
27. C. VERDON, A. KARIMI and J.-L. MARTIN, *Mater. Sci. Eng.* A **245** (1998) 11.
28. C.-J. LI, A. OHMORI and Y. HARADA, *J. Therm. Spray Technol.* **5**(1) (1996) 69.
29. M. L. LAU, H. G. JIANG, W. NUCHTER and E. J. LAVERNIA, *Phys. Stat. Sol.* (a) **166** (1998) 257.
30. L. PAWLOWSKI, in "The Science and Engineering of Thermal Spray Coatings" (John Wiley & Sons Ltd, Chichester, England, 1995) p. 210.
31. J. HE, M. ICE, S. DALLEK and E. J. LAVERNIA, *Metall. Mater. Trans.* **31**A(2) (2000) 541.
32. C. HERRING, *J. Appl. Phys.* **21** (1950) 301.
33. G. GILLE and B. SZESNY and G. LEITNER, *J. Advanced Mater.* **31**(2) (1999) 9.
34. B. K. KIM, G. H. HA and D. W. LEE, *J. Mater. Processing Technol.* **63** (1997) 317.

Received 20 September 2001
and accepted 24 April 2002